2

Nanostructures Fabricated by Laser Techniques for Sensors Applications

Aurelian Marcu, Cristian Viespe[*]

Atomistilor 409, Bucharest-Maguree, Romania
[*]Corresponding author

Outline:

Introduction.. 30
Vapor-Liquid-Solid technique.. 30
Pulsed-Laser-Deposition technique.. 31
Surface-Acoustic-Wave sensors.. 32
Types of Nanostructures in sensors applications.. 33
Nanoparticles in SAW sensors.. 33
Nanowires in SAW sensors.. 35
Micropatterned Nanostructured areas in SAW sensors.. 35
Conclusions.. 37
Acknowledgments.. 37
References.. 37

Introduction

The advance of micro and nanotechnologies requires materials and surfaces with continuously improved properties. It is known that the properties of the materials are dramatically changing from macro to micro dimensions and in the nanometric ranges many of them became size-dependent properties (E.G. luminescence [1], mechanical properties [2], magnetic properties [3] and so on). Thus, while talking about nanostructured surfaces, beside material crystalline structure, nanostructure morphology and respectively structure shape and morphology control became a crucial factor in surface and fabricated device performances. Sensors and particularly Surface Acoustic Wave (SAW) sensors are one of the examples of such applications.
There are generically two approaches in nanostructure fabrication, by so called 'Top-Down' and respectively 'Bottom-Up" techniques. However, due to the costs and technological limitations, Bottom-Up approaches are the only 'effective' options when it came to device applications, and SAW sensor application is not an exception. There are several ways of controlling the dimensions and properties of the fabricated structures, and the catalyst based fabrication from the vapor-Liquid-Solid (VLS) technique is one of the approaches which give a good controllability over the nanostructure morphology and structure. While chemical methods give a good productivity, the laser based methods give the advantages of a contaminant free approach - which particularly for sensor application is again a crucial future - and very good structural parameter control. Thus, Pulsed Laser Deposition technique (PLD) combined with VLS technique is among the best approaches for the nanostructure fabrication from the nanostructure parameters control point of view. We will further present some general descriptions of the fabrication techniques and the corresponding nanostructure morphology and properties control used in sensor applications

Vapor-Liquid-Solid technique

VLS becomes one of the most popular bottoms up nanostructure fabrication techniques. A liquid eutectic droplet catalyses capture material from the vapour (Fig. 2.1) and incorporate it into the solid (Fig. 2.5) [4] so, the formed nanostructure (in this case nanowire) dimensions are generally controlled by the catalyst size: droplet diameter will control the wire diameter and growing time will determine the nanowire length. This technique is particularly used for oxide materials [5, 6, 7, 8, 9, 10], but not exclusively [11, 12]. Specific to this technique is the fact that the incoming material is not deposited (growing) everywhere on the surface, but preferentially collected and grown within the catalyst droplets. For this reason the catalyst material should have a chemical composition which will make no reaction with the grown material (or with the substrate one). Thus, 'noble materials' are commonly used as catalysts and gold is probably the most popular option among them.
As could be seen in Fig. 2.5, the growing process is taking place within the droplet and cumulates both straight incoming particles as vapors (I) and surface diffused ones (D), but excluding the droplet desorbed particle flux (E). Thus, as a global equation for the mass (and respectively particle fluxes) inside the catalyst droplet it could be written:

$$V = I + D - E \tag{1}$$

where V is the deposited particle flux, I am the direct incoming flux, D is the diffused flux and E is the droplet desorption flux.

Deposition process inside the catalyst droplet is generally considered as an “instantaneous” process after particles reach a “critical concentration” inside it. However, growing speed has to be limited between some minimal and maximal growing speed limitations generated by desorption process and the particle movement and nucleation limitations within the liquid. While the minimum particle flux limitation has been already experimentally confirmed for oxide materials [13] the incoming particle flux is generally accepted as necessary to be below a particular limit (usually unlikely to be reached within regular deposition conditions).

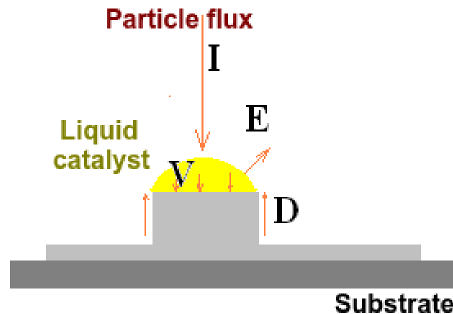

FIGURE 2.1
Vapor-Liguid-Solid (VLS) growing mechanism

Some more limitations in the VLS growing process, are related to the catalyst size [12], incoming particle size [14], or surface temperature to insure the diffusion process or particle flux incoming directions [15] and so on.

Pulsed-Laser-Deposition technique

For the synthesis of various materials, pulsed laser deposition (PLD) has been one of the most powerful techniques to fabricate films and nanostructures as well [16, 17, 18, 19, 20] using different system geometries [21, 22]. A 'standard' experimental setup of a PLD system is presented in Fig. 2.2. The laser beam irradiates a target and the generated plume is captured on a substrate surface placed in front of the target. In order to uniformly ablate the entire surface of the target, the target holder is usually describing 1D or 2D movements.
During plasma expansion, the particles interacts each other. Depending on the ambient gas composition and pressure, they could aggregate forming nanoparticles. This is actually one of the techniques for nanoparticle formation using laser ablation [23]. On the other hand, when the application requests a controlled particle size generation (and the VLS is one of them) depending on the laser parameters and respectively laser-matter interaction process some special plume filtering techniques have to be used. Such techniques are usually implemented in special system geometries and are based on 'big particles' 'ballistic' trajectories. Among used techniques, we should mention plane shadow masks [20, 24] as having the simplest setups, and helical masks [20, 25] as insuring the best particle size control (while plume particles penetrate through the mask's elements instead of 'surrounding' it) while the plasma reflection [26] is an easy technique having the best fluency performance filtration among these techniques.

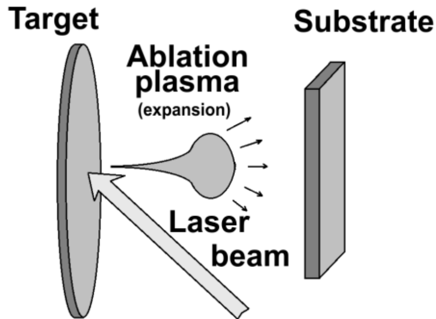

FIGURE 2.2
Experimental setup and plasma expansion in Pulsed-Laser Deposition systems

PLD combined with the VLS technique insure a good nanostructure crystalline structure [27] as well as a good morphology and structure property control [28].

Surface-Acoustic-Wave sensors

SAW sensors are one of the most promising detection systems due to smaller size, lower weight, power requirements and great sensitivity. The control of the nanostructure morphological and structural properties is an essential point in SAW sensors.
A surface acoustic wave sensor generally consists in a piezoelectric substrate, a pair of the interdigital transducers (IDTs) and an ad/ absorbent film (Fig. 2.3). The electrical signal connected to one of the transducers (input) generates a SAW which propagates towards the other transducer, the mechanical wave being converted into an electrical signal. The acoustic wave undergoes a delay and frequency modification, which depends on the substrate piezoelectric material, the distance between the transducers and the chemical sensitive film characteristics.
A SAW type sensor operates on the following principle: any modification of the mass or visco-elastic properties of the sensitive receptor material in the device, leads to a frequency change and amplitude, which can be correlated with the physical quantity being measured.

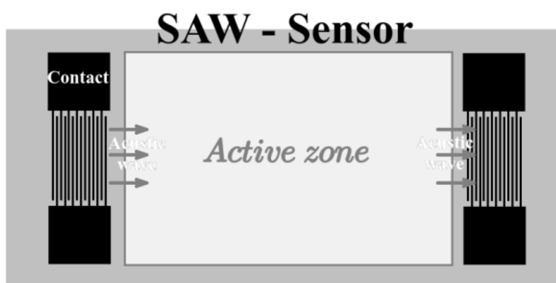

FIGURE 2.3
Surface acoustic wave sensor

The oscillating system of SAW sensors (Fig 2.4), in general, includes an amplifier (in order to compensate the signal lose in the circuit), a band-pass filter (to cut the spurious oscillation at unwanted frequency), a phase shifter (to adjust the round-trip phase shift of the circuit) and a frequency counter. The arrangement of components in the loop is also important. For example, a

band-pass filter placed just after the amplifier, removes any harmonics generated by an amplifier that can "confuse" the frequency counter.

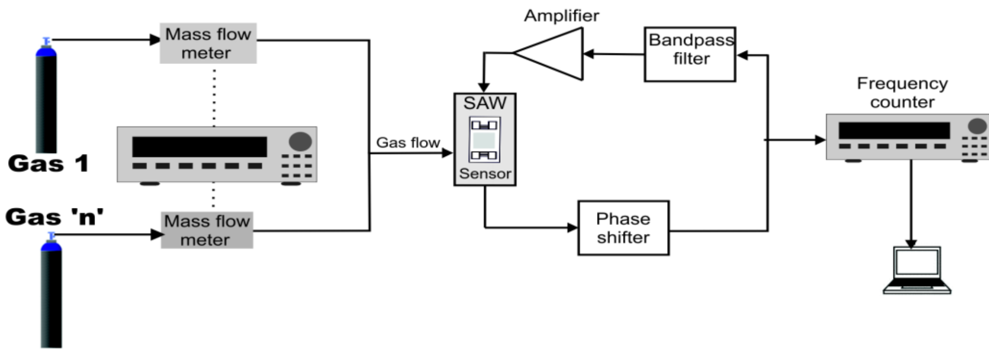

FIGURE 2.4
SAW sensor measurement setup

As a surface acoustic wave sensor to oscillate stable, it must generally meet two conditions:
(1) Signal returns after all crossed loops (band-pass filter, phase shifter, amplifier) at the starting point with the same amplitude.
(2) The phase shift is a multiple of 2π.
Conditions (1) and (2) are simultaneously satisfied if the amplifier has a gain greater than or equal to the insertion loss of the circuit and phase is zero.

Types of Nanostructures in sensor applications

It has been demonstrated that nanostructured materials possess enhanced performance properties compared to bulk materials when they are used in similar applications and could change their properties as a function of size and structure [1]. Sensors using nanoparticles [29, 30, 31], nanowires [32, 33, 34], nanoporous materials [35, 36, 37] and micropatterned nanostructure [38] have enhanced absorption properties, mainly due to the increased surface area of the nanoscale materials. In general, nanoparticle covered active surfaces are easy to prepare, and have a good response to a large range of gas concentrations, nanoparticle active layers benefit of a very large surface area due to the high surface/volume ratio, while the (oriented) nanowire active surfaces have a very good property control and a large accessibility of the surface by the monitored gases/fluids.

Nanoparticles in SAW sensors

It has been demonstrated that the structure of the SAW films represents a parameter that control the sensors performance [39]. Nanostructure porosity induces a rapid diffusion of gases in and out of the films, and a greater surface area increases the sensitivity. For this reason nanoparticles could be used for increasing the surface area. C. Viespe et al [40] made a comparative study between sensitive layers based on nanoparticles, with diameters of 2-15 nm, of SiO_2, TiO_2, TiN and Co_3N, embedded in polyethyelenimine (PEI). The sensors were used for detection of chloropicrin, soman

and levisite. In table 2.1 are presented the sensitivity and limit of detection for sensors with PEI, SiO_2 -PEI, TiO_2 - PEI, TiN- PEI and Co_3N-PEI.

TABLE 2.1
Sensitivity and LOD (Δf = frequency deviation; f = frequency oscillation)

Chemical Gas	Polymer type	Sensibility Δf/c (Hz/ppm)	LOD (ppm)
chloropicrin	SiO_2/Si -PEI	0.17	535
	TiN-PEI	0.1	862
	TiO_2-PEI	0.09	1035
	Co_3N-PEI	0.12	739
soman	SiO_2/Si-PEI	0.53	170
	TiN-PEI	0.31	293
	TiO_2-PEI	0.27	334
	Co_3N-PEI	0.23	391
levizita	SiO_2/Si-PEI	1.36	66
	TiN-PEI	0.98	92
	TiO_2-PEI	0.71	103
	Co_3N-PEI	2.31	39

Figure 2.5 shows SEM images of the surface film nanocomposite. As seen, nanoparticles with sizes below 15 nm are randomly distributed over the entire surface. (Cracks in the film are produced during the SEM investigations due to surface heating by the electron beam). The film thickness is around 450 nm.

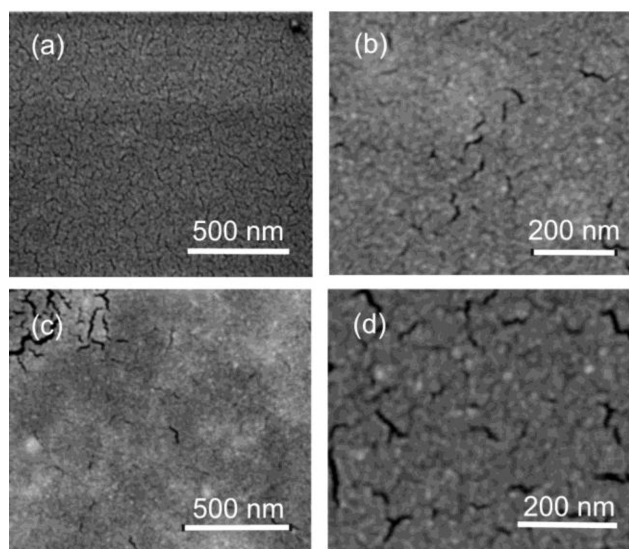

FIGURE 2.5
SEM image of the sensitive layer (a) SiO2/Si-PEI; (b) TiN-PEI; (c) TiO2-PEI; (d) Co3N-PEI

Nanowires in SAW sensors

Unlike the nanoporous or nanoparticles active layers, nanowires could present a more organized and controlled surface morphology and properties. This could insure a more “effective” active surface and respectively a faster response of the sensors for lower concentrations of the monitored gases (or liquids). As could be seen in the Fig 2.6 below, the structures are fully accessible from the ambient atmosphere due to the fact they are grown vertically aligned on the sensor active surface area. Thus, in the presented case, for 20-40 nm diameter nanowires, 500 nm long and just a 25% surface “covering factor” (percentage of the active surface area covered by nanowires), the active surface area will be already tens of times bigger than the same sensor area covered by a plane film, while the deposited volume of material will be fully penetrated for just 10-20 nm (monitored) gas penetration depth. Our investigations have pointed out that the nanowire sensor detection limit could easily go with one order below the film based sensor limit [33] in similar conditions. However, nanowire based sensors will be much faster saturated at high gas (hydrogen in our case) concentrations, making this morphology more effective for monitoring lower gas concentrations.

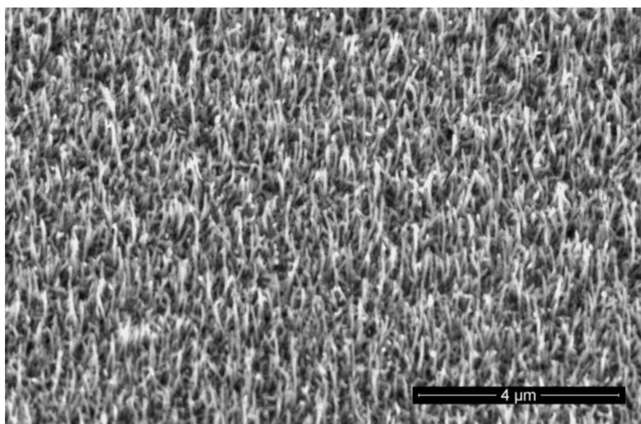

FIGURE 2.6
Morphology of the laser-grown (PLD/VLS) nanowire on the active surface area of SAW sensors

Micropatterned Nanostructured areas in SAW sensors

Nanopatterning influences were investigated by growing nanowires on same percent of the sensors active areas, nanowires with same morphology and structural properties, with the only difference in the shape of the grown area. Thus as could be seen in Fig. 2.7, the surface of a 1 cm x 1 cm square area was also grown as perpendicular and longitudinal, straight and bended stripes. In spite of the same covered area and same nanostruture morphologies and structural properties, the sensor response was different in terms of sensibility.

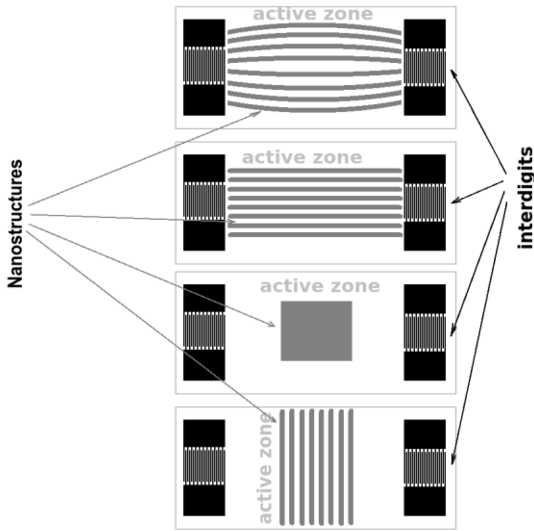

FIGURE 2.7
Nanostructure covered active surface zone patterning on SAW sensor

The main difference induced by the pattern over the active surface area response seems to be in the sensor noise, and it is controlled by the interaction between the surface waves and the nanowire deposited patterns. In order to prove this, the noise of these four patterns was monitored while adding auxiliary ZnO layers (as a thin film) over the whole sensor active areas. As could be seen in Fig. 2.8 the noise of the sensor is increasing with the deposited auxiliary layer (together with the sensor response) and its end-up to a common value for all of them, value specific to a thin film sensor performance [31]

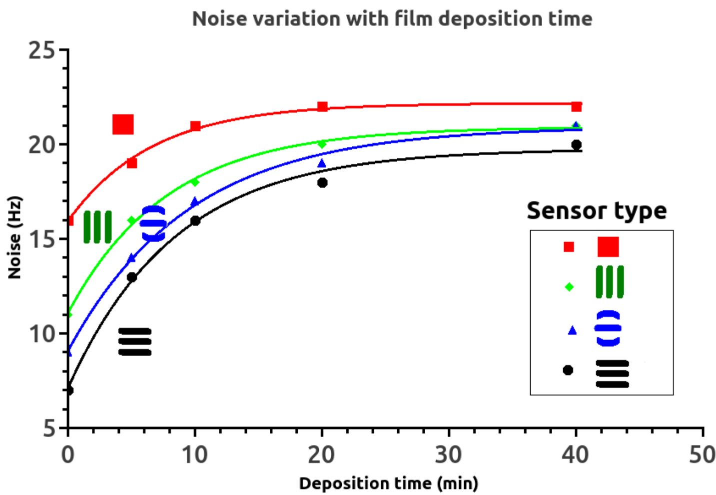

FIGURE 2.8
The sensor noise variation on the thin film thickness over the nanowire patterns

Conclusion

Nanowire seems to be the best morphological options for the active surface area morphology, due to the high surface area and the low amount of the deposited material. The main advantage of these structures is the enhancement of the detection limit and response speed through the high surface/volume ratio. However, these structures will easily saturate at high gas concentrations making these structures suitable mostly for monitoring low concentration gases.

Acknowledgement

This work was supported by a grant of the Romanian National Authority for Scientific Research, CNCS—UEFISCDI, projects numbers LAPLAS 4 PN 09 39 01 05, PN-II-PT-PCCA-2011-3.2-0762 and PN-II-RU-TE-2014-4-0342.

References

1. A. Marcu, C. Sima, C. Grigoriu, I. Enculescu and B. Iliescu, Journal of Optoelectronics and Advanced Materials, 10 (2008) pp. 3131 – 3134 1
2. J. Liu, L.-L. Wang, J. Lee, R. Chen, O. El-Fakir, L. Chen, J. Lin, T. A. Dean, J. Mat. Proc. Tech. 224 (2015), pp. 169–180
3. W. S. Seo, H. H. Jo, K. Lee, B. Kim, S. J. Oh, and J. T. Park, Angew. Chem. 2004, 116, pp. 1135 –1135
4. R. S. Wagner, W. C. Ellis, Appl. Phys. Lett. 4 (1964) 89.
5. L. Yuguo, Y. Aichun, Z. Boshi, P. Ruiqin, Z. Xuelei, J. Semicond. 32 (2011) 023002
6. J. C. Lee, K. S. Park, T. G. Kim, H. J. Choi, Y. M. Sung, Nanotechnology 17 (2006) 4317.
7. H. Srivastava, P. Tiwari, A. K. Srivastava, R. V. Nandedkar, J. Appl. Phys. 102 (2007) 054303.
8. H. W. Kim, J. W. Lee, Physica E 40 (2008) 2499.
9. H. W. Kim, S. H. Shim, Chem. Phys. Lett. 422 (2006) 165.
10. Q. Wan, E. N. Dattoli, W. Y. Fung, W. Guo, Y. Chen, X. Pan, W. Lu, Nano Lett. 12 (2006) 2909.
11. K. Tateno, G. Zhang, H. Nakano, Nano Lett. 8 (2008) 3645.
12. A. Marcu, L. Trupina, R. Zamani, J. Arbiol, C. Grigoriu and J. R. Morante, Thin. Solid Films 520 (2012), pp. 4626 – 4631, online (2011)
13. A. Marcu, T. Yanagida, K. Nagashima, H. Tanaka and T. Kawai, Journal of Applied Physics, 102 (2007) pp.016102
14. A. Marcu, C. Grigoriu, C. P. Lungu, T. Yanagida and T. Kawai, Phys. E 44, (2012) pp. 1071-1073
15. A. Marcu, F. Stocker, R. R. Zamani and C. P. Lungu, Appl. Surf. Sci, 327 (2015). pp 262–267
16. A. Marcu, L. Trupina, R. Zamani, J. Arbiol, C. Grigoriu and J. R. Morante, Thin. Solid Films 520 (2012), pp. 4626 – 4631, online (2011)
17. A. Marcu, M. Goyat, T. Yanagida and T. Kawai, Journal of Optoelectronics and Advanced Materials 11 (2009), pp. 421-426
18. F. Dumitrache, I. Morjan, R. Alexandrescu, V. Ciupina, G. Prodanb, I. Voicu, C. Fleaca, L. Albu, M. Savoiu, I. Sandu, R. Popovici, I. Soare, Applied Surface Science 247 (2005) 25–31.

19. I. Morjan, R. Alexandrescu, I. Soare, F. Dumitrache, I. Sandu, I. Voicu, A. Crunteanu, E. Vasile, V. Ciupina, S. Martelli, Materials Science and Engineering C23 (2003) 211–216.
20. A. Marcu, C. Grigoriu, W. Jiang and K. Yatsui, Thin Solid Films, 360 (2000), pp.166-172
21. A. Marcu, F. Stocker, R. R. Zamani and C. P. Lungu, Appl. Surf. Sci, 327 (2015). pp 262–267
22. A. Marcu, C. Grigoriu and K. Yatsui, Applied Surface Science, Vol 252 (2006), pp. 4733
23. C. Grigoriu, I. Nicolae, V. Ciupina, G. Prodan, H. Suematsu, and K. Yatsui, J. Optolectron. Adv. Mat. 6, 825 (2004)
24. A. Marcu, C. Grigoriu, C. P. Lungu, T. Yanagida and T. Kawai, Phys. E 44, (2012) pp. 1071-1073,
25. A. Marcu, M. Goyat, T. Yanagida and T. Kawai, Journal of Optoelectronics and Advanced Materials 11 (2009), pp. 421-426
26. A. Marcu, C. Grigoriu and K. Yatsui, Applied Surface Science, Vol 248 (2005), pp. 466-469
27. A. Marcu, C. Sima, C. Grigoriu, I. Enculescu and B. Iliescu, Journal of Optoelectronics and Advanced Materials, 10 (2008) pp. 3131 – 313
28. A. Marcu, T. Yanagida, K. Nagashima, H. Tanaka and T. Kawai, Journal of Applied Physics, 102 (2007) pp.016102
29. D. Sil, J. Hines, U. Udeoyo, E Borguet, ACS Appl. Mater. Interfaces 7 2015 5709–5714.
30. C. Viespe, C. Grigoriu, Sens. Actuators B: Chem. 147 (2010) 43-47.
31. D. T. Phan, G. S. Chung, Sens. Actuators B: Chem. 20-23 161 (2012) 341–348.
32. A. Marcu, C. Viespe, Sens. Actuators B: Chem 208 (2015) 1-6.
33. M. Z. Atashbar, K. Kalantar-zadehm, S. J. Ippolitto, W. Wlodarski, 2005 IEEE Sensors, 1 and 2, (2005) 1363–1365.
34. W. Peng, Y. He, C. Wen, K. Ma, Sens. Actuators A: Phys. 184 (2012) 34-40.
35. L. Al-Mashat, D. S. Ahn, S. H. Han, W. G. Hong, K. Shin, C. S. Yoon, K. Kalantar-Zadeh, W. Wlodarski, Sensor Letters, 9 1 (2011) 73-76.
36. C. Viespe, C. Grigoriu, Microelectronic Engineering, 108, (2013) 218-221.
37. O. K. Varghese, D. Gong, W. R. Dreschel, K. G. Ong, C. A. Grimes, Sens. Actuators B: Chem. 94, 1 (2003) 27-35.
38. A. Marcu, N. Ionut, C. Viespe, Sensors & Actuators: B. Chemical, 10.1016/j.snb.2016.03.015
39. A. Marcu, C. Grigoriu and K. Yatsui, Applied Surface Science, Vol 248 (2005), pp. 466-469.
40. C. Viespe, C. Grigoriu, C. Toader, I. M. Popescu, UPB Sci. Bull., Series A, Vol. 73, Iss.1, 2011